Reversing CdS and ZnS preparation order on electrospun TiO_2 and its effects on photoelectrochemical property

Yue Li ✉, *Fengxian Gao, Longtao Zhao, Yingjie Ye, Jian Liu, Yanzhong Tao*

School of Materials and Chemical Engineering, Henan Institute of Engineering, Zhengzhou, Henan 451191, People's Republic of China
✉ *E-mail: liyue0128@163.com*

Published in Micro & Nano Letters; Received on 14th March 2016; Revised on 9th June 2016; Accepted on 26th July 2016

CdS and ZnS co-sensitised one-dimensional TiO_2 nanofibres were successfully prepared by a combination of electrospinning and successive ionic layer adsorption and reaction (SILAR) process because both electrospinning and SILAR method are inexpensive and scalable techniques. The composites of CdS-ZnS/TiO_2 heterojunctions were compared with electrode containing only CdS being superior in terms of photoelectrochemical tests. The results showed that the photocurrent of CdS-ZnS/TiO_2 nanofibres was seven times than that of CdS/TiO_2 nanofibres and seven times than that of pure TiO_2 nanofibres. The increased photocurrent is depended on the preparation order of ZnS and CdS on TiO_2 nanofibres.

1. Introduction: Since the water splitting property of TiO_2 was discovered by Fujishima and Honda almost 40 years ago [1], the photocatalytic properties of TiO_2 have been widely studied due to the advantages of low cost, stability and non-toxicity under the irradiation of ultraviolet light [2–4]. Recently, one-dimensional (1D) TiO_2 nanostructures have attracted increased attention because of their enlarged surface areas and reduced diffusion lengths compared with conventional TiO_2 materials [5]. Inspiringly, several techniques have been developed for generating nanoscale wires, belts, and tubes such as template growth [6], self-assembling [7], thermal evaporation [8], solvothermal synthesis [9] and so on. Electrospinning is a well-known and economical technique used for large-scale fabricating 1D fibres by combination with the sol–gel technique. [10]. One of the attractive features of this method is that the technique could build the new platform for fabricating 1D fibres with diameters ranging from nanoscale to microscale in possession of great length and high specific surface area. However, the photocatalytic efficiency of TiO_2 nanocatalysts is limited because of the high band gap (3.2 eV) and the fast recombination rate of photogenerated electrons and holes [11]. Subsequently, the development of TiO_2-based photoelectrocatalyst with visible light response has become a research focus [12, 13].

Motivated by the above concerns, we reported a novel nanostructure of electrospun CdS-ZnS/TiO_2 heterojunction by combining the electrospinning technique and the successive ionic layer adsorption and reaction method (SILAR). CdS have been paid much more attention because of their high potential in the light harvest in a visible light region. However, pure CdS is generally not very active due to the disadvantage of photocorrosion [14]. One way to improve the stability and photoactivity is to develop composite nanostructures by incorporating a wide bandgap semiconductor (such as ZnS has a wide band gap of 3.67 eV) [15]. Thus, TiO_2 co-sensitised by CdS and ZnS provide superior abilities: (i) extending the light adsorption spectrum and improving the using efficiency of visible light, (ii) suppressing the recombination of photogenerated electron/hole pairs, and (iii) suppressing the photocorrosion of CdS. We also found the preparation order of CdS and ZnS has a great influence on the photoelectrochemical property. The modified TiO_2 nanofibres by first deposition ZnS redeposition CdS exhibited much higher photocurrent value than the samples prepared by opposite order.

2. Experiment: TiO_2 (P25, 20% rutile and 80% anatase) was purchased from Degussa. Poly (vinylpyrrolidone) (PVP; Mw = 1,300,000) was purchased from Alfa Aesar. Absolute ethanol, acetic acid, $Cd(NO_3)_2$, $Zn(NO_3)_2$, and Na_2S were supplied by Beijing Chemical Reagent Plant (Beijing, China) and used as received without further purification. The water used was ultrapure. The experiments were carried out at room temperature and humidity.

The TiO_2 nanofibres were fabricated by electrospinning a mixture of TiO_2 sol and PVP polymer. Typically, 1.5 g of titanium tetraisopropoxide ($Ti(O^iPr)_4$) was dissolved in a mixture of 3 ml ethanol and 3 ml acetic acid by stirring for 1 h to obtain the TiO_2 sol. Then, 0.45 g of PVP dissolved in 3 ml ethanol was added to the TiO_2 sol solution and stirred for 3 h. After that the prepared precursor solution placed in a hypodermic syringe for electrospinning. An electrical potential of 10 kV was applied between the metallic nozzle and the aluminium foil collector at a distance of 15 cm. The as-collected nanofibres were calcined at 450°C for 3 h to remove the remaining PVP and to obtain the anatase TiO_2 nanofibres.

TiO_2 nanofibres were sensitised with ZnS and CdS using previously reported SILAR methods. In a typical procedure, the TiO_2 nanofibres were dipped into a solution containing 0.2 M $Zn(NO_3)_2$ in ethanol for 1 min, rinsed with deionised water, and then immersed into a solution containing 0.2 M Na_2S solution in methanol for 1 min followed by another rinsing with deionised water. Such a process was repeated five times to get a suitable ZnS coating on the TiO_2 electrode. CdS was also deposited onto the ZnS/TiO_2 electrode by the same method using 0.2 M $Zn(NO_3)_2$ and 0.2 M Na_2S. Five step SILAR cycles were repeated to get a suitable CdS coating on the ZnS/TiO_2 electrode. The product was named as CdS-ZnS/TiO_2 nanofibres. For comparison, the immersion order was five cycles for CdS and then five cycles for ZnS, which was labelled as ZnS-CdS/TiO_2 nanofibres. The prepared route is schematically shown in Fig. 1.

The morphologies of the samples were studied using a field-emission scanning electron microscope (FE-SEM; Hitachi S-4800, 5 KV) and high-resolution transmission electron microscopy (HRTEM; JEOL JEM-2100F). Energy dispersive spectroscopy (EDS) attached to the TEM was employed to analyse the composition of the structure. The crystal phases were determined by X-ray diffractometer (XRD) recorded by a Rigaku Dmax 2200 XRD equipped with Cu-Ka radiation (λ). Diffuse reflectance

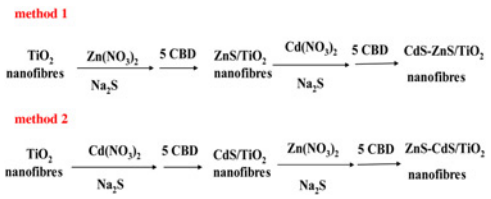

Fig. 1 *Scheme shows the prepared products by different methods*

absorption spectra (DRS) were obtained on using a Hitachi U-3010 spectroscopy with $BaSO_4$ as a reference.

Photoelectrochemical studies were carried out with a CHI 660C electrochemical analyser (CHI Inc., USA.) in a three-electrode configuration. The as-prepared samples were used as the working electrode, a platinum wire as the counter electrode, and an Ag/AgCl (KCl saturated) electrode as the reference electrode in 1.0 M KOH solution as the electrolytes. Samples were tested in a quartz cell under simulated solar light from a 500 W xenon arc lamp (Beijing Changtuo). The incident light intensity was 74 mW/cm^2 measured by a radiometer (FZ-A, Photoelectric Instrument Factory of Beijing Normal University, China).

3. Results and discussion: The surface morphology of the CdS-ZnS/TiO_2 nanofibres was studied by FE-SEM and TEM measurements. Fig. 2*a* shows a large area SEM image of the pure electrospun TiO_2 nanofibres. It was showed that these randomly oriented TiO_2 had a smooth and uniform surface without secondary nanostructures, and the average diameter of the nanofibres ranging from 120 to 250 nm. After sensitising by SILAR methods, the surface of as-fabricated samples was no longer smooth instead of decorating with a bundle of nanowires (shown in Fig. 2*b*). The microstructure was also analysed by TEM studies, shown in Fig. 2*c*, the unsmooth surface of the CdS-ZnS/TiO_2 nanofibres was agreement with the SEM image of Fig. 2*b*. The corresponding EDX spectrum in Fig. 2*d* reveals that the obtained composite product is composed of Ti, O, Cd, Zn and S. The calculated molar percentages of Cd, Zn and S are about 7.47, 7.70 and 14.86%, respectively. The total amount of Cd and Zn are nearly equal to the amount of S, being in line with the molar ratio of CdS and ZnS.

The XRD patterns in Fig. 3 show the characteristic peaks of unmodified TiO_2 nanofibres and the CdS-ZnS/TiO_2 nanofibres to further confirm the existence of TiO_2, CdS and ZnS. The TiO_2 in

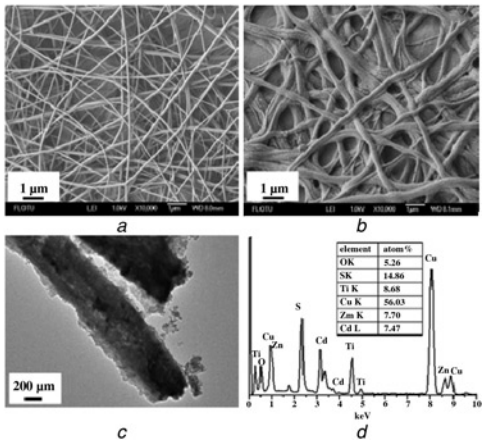

Fig. 2 *SEM, TEM and EDS images of the samples*
a SEM image of TiO_2 nanofibres
b SEM image of CdS-ZnS/TiO_2 nanofibres
c TEM micrograph of CdS-ZnS/TiO_2 nanofibres
d EDX pattern of the composite nanofibres

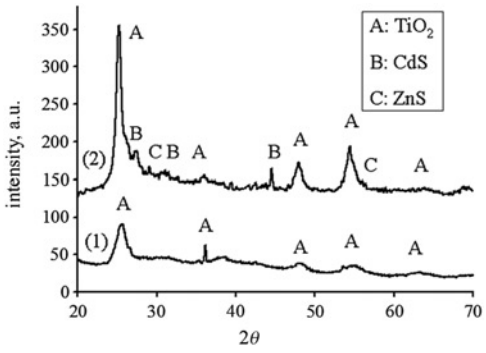

Fig. 3 *XRD pattern of the samples: (1) TiO_2 nanofibres and (2) CdS-ZnS/TiO_2 nanofibres*

curve (1) showed the peaks assigned to the anatase phase (JACPDS 21-1272). Compared with curve (1), additional peaks appeared in curve (2) were attributed to ZnS and CdS phase. The 2θ values of 28.8° and 56.8° assigned to the (111), (220) planes of ZnS (JACPDS 05-0566), while the characteristic diffraction peaks at 26.5°, 30.6° and 43.9°, corresponding to the (111), (200) and (220) planes of CdS (JACPDS 65-2887).

The DRS of TiO_2 nanofibres, CdS/TiO_2 nanofibres, ZnS-CdS/TiO_2 nanofibres and CdS-ZnS/TiO_2 nanofibres were shown in Fig. 4. The absorption edge of pure TiO_2 nanofibres was observed at about 400 nm, corresponding to the band-gap energy of 3.0 eV. The band gap energy can be estimated by the equation of $a = A(h\upsilon - Eg)^{n/2}/h\upsilon$, where A is a constant, h is the Planck's constant, Eg is band energy, υ is the frequency of the incident light, and n is equal to 1 for the direct transition [16]. The intercept of the tangent to the plot in the inset of Fig. 4 showed the band gaps of CdS/TiO_2 nanofibres were corresponding to 2.8 eV. After co-sensitised ZnS and CdS, the band gap reduced to about 2.6 eV. The similar value on CdS-ZnS/TiO_2 nanofibres and ZnS-CdS/TiO_2 indicates that the deposition order of ZnS and CdS has not great influence on the ability of harvesting visible light. However, the modification of both CdS and ZnS on TiO_2 nanofibres resulted in a significant enhancement in absorption in visible range as compared with TiO_2 nanofibre or CdS/TiO_2 nanofibres. This result suggests the possibility of using the co-sensitised materials on generating photocurrent with lower energetic requirements than TiO_2.

Fig. 5 shows photocurrent generated from unmodified TiO_2, CdS/TiO_2, CdS-ZnS/TiO_2 nanofibres and ZnS-CdS/TiO_2 nanofibres upon visible light excitation. The electrode responds promptly to light on/off. The value of photocurrent density was about 0.37 mA/cm^2 for CdS-ZnS/TiO_2 nanofibres, which was more than nine

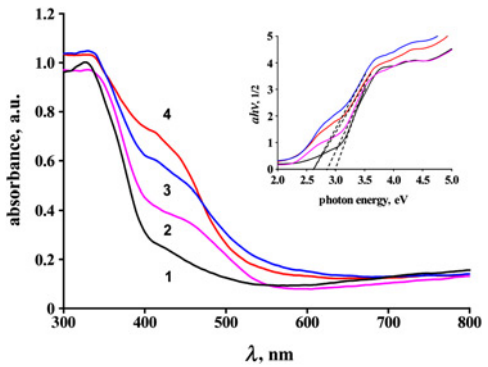

Fig. 4 *UV-vis DRS of (1) TiO_2 nanofibres, (2) CdS/TiO_2 nanofibres, (3) ZnS-CdS/TiO_2 nanofibres, and (4) CdS-ZnS/TiO_2 nanofibres. The inset shows the corresponding plots of $(ah\upsilon)^2$ against photon energy*

doi: 10.1049/mnl.2016.0134

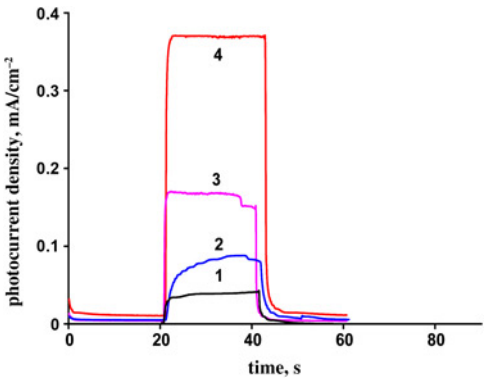

Fig. 5 *Photocurrent responses of (1) TiO_2 nanofibres, (2) ZnS-CdS/TiO_2 nanofibres, (3) CdS/TiO_2 nanofibres, and (4) CdS-ZnS/TiO_2 nanofibres (Intensity: 100 mW/cm^2; electrolyte: 1 M KOH)*

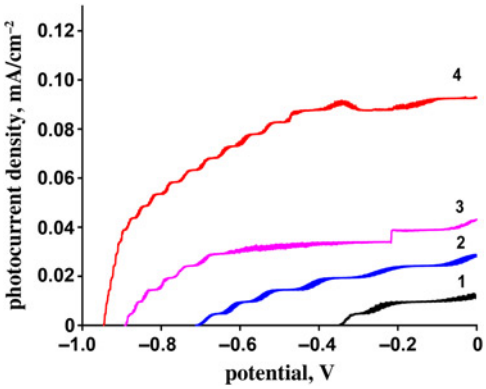

Fig. 6 *I–V characteristics for (1) TiO_2 nanofibres, (2) ZnS-CdS/TiO_2 nanofibres, (3) CdS/TiO_2 nanofibres, and (4) CdS-ZnS/TiO_2 nanofibres (Intensity: 100 mW/cm^2; electrolyte: 1 M KOH, potential: V against Ag/AgCl)*

times higher than that of the unmodified TiO_2 nanofibres (0.04 mA/cm^2) and two times higher than that of the CdS/TiO_2 nanofibres (0.17 mA/cm^2). The results indicated the fastest separation efficiency of photoinduced electrons and holes and increased lifetime of the charge carriers on co-sensitised CdS-ZnS/TiO_2 nanofibres. However, after reversing the preparation order of ZnS and CdS, the result was quite different from the previous one. The photocurrent of ZnS-CdS/TiO_2 nanofibres became very low, even lower than that of CdS/TiO_2 nanofibres. The detailed reason for this phenomenon is not clearly, while the similar results happened on CdS-Pt/TiO_2 system [17].

I–V characteristics also confirmed the above result. Higher open-circuit photovoltage means faster electrons and holes separation efficiency and thus better performance on photoelectrochemical test [18]. Accordingly, as shown in Fig. 6, the CdS-ZnS/TiO_2 nanofibres were obviously higher than the ZnS-CdS/TiO_2 nanofibres, indicating CdS-ZnS/TiO_2 nanofibres were far more efficient than ZnS-CdS/TiO_2 nanofibres. In such cases, the photocurrent collection efficiency correlated with the preparation order of ZnS and CdS on TiO_2 nanofibres.

4. Conclusion: The photoelectrochemical performance of CdS and ZnS co-sensitised TiO_2 nanofibres were investigated. The co-sensitised TiO_2 nanofibres significantly enhanced the visible light response of the electrodes. The CdS-ZnS/TiO_2 nanofibres showed highest photocurrent, and consequently highest photoelectrochemical activity as compared with CdS/TiO_2 nanofibres and unmodified TiO_2 nanofibres. However, the result was greatly changed by reversing the deposition order of ZnS and CdS, only depositing the ZnS first and then the CdS could get the better result.

5. Acknowledgments: This research was supported by the Doctor Foundation of Henan Institute of Engineering (D2015020).

6 References

[1] Fujishima A., Honda K.: 'Electrochemical photolysis of water at a semiconductor electrode', *Nature*, 1972, **238**, (238), pp. 8–37

[2] Xiong Z., Zhao X.: 'Titanate@TiO_2 core-shell nanobelts with an enhanced photocatalytic activity', *J. Mater. Chem. A*, 2013, **1**, (26), pp. 7738–7744

[3] Fang J., Xu L., Zhang Z., *ET AL.*: 'Au@TiO_2–CdS ternary nanostructures for efficient visible-light-driven hydrogen generation', *ACS Appl. Mater. Interfaces*, 2013, **5**, (16), pp. 8088–8092

[4] Liao J., Lin S., Zhang L., *ET AL.*: 'Photocatalytic degradation of methyl orange using a TiO_2/Ti mesh electrode with 3D nanotube arrays', *ACS Appl. Mater. Interfaces*, 2011, **4**, (1), pp. 171–177

[5] Hwang Y.J., Hahn C., Liu B., *ET AL.*: 'Photoelectrochemical properties of TiO_2 nanowire arrays: a study of the dependence on length and atomic layer deposition coating', *ACS Nano*, 2012, **6**, (6), pp. 5060–5069

[6] Foong T.R., Shen Y., Hu X., *ET AL.*: 'Template-directed liquid ALD growth of TiO_2 nanotube arrays: properties and potential in photovoltaic devices', *Adv. Funct. Mater.*, 2010, **20**, (9), pp. 1390–1396

[7] Liu J., Bai H., Wang Y., *ET AL.*: 'Self-assembling TiO_2 nanorods on large graphene oxide sheets at a two-phase interface and their anti-recombination in photocatalytic applications', *Adv. Funct. Mater.*, 2010, **20**, (23), pp. 4175–4181

[8] Wu J.-M., Shih H.C., Wu W.-T.: 'Formation and photoluminescence of single-crystalline rutile TiO_2 nanowires synthesized by thermal evaporation', *Nanotechnology*, 2005, **17**, (1), p. 105

[9] Yang H.G., Liu G., Qiao S.Z., *ET AL.*: 'Solvothermal synthesis and photoreactivity of anatase TiO_2 nanosheets with dominant {001} facets', *J. Am. Chem. Soc.*, 2009, **131**, (11), pp. 4078–4083

[10] Kim I.-D., Rothschild A., Lee B.H., *ET AL.*: 'Ultrasensitive chemiresistors based on electrospun TiO_2 nanofibres', *Nano Lett.*, 2006, **6**, (9), pp. 2009–2013

[11] Peining Z., Nair A.S., Shengjie P., *ET AL.*: 'Facile fabrication of TiO_2–graphene composite with enhanced photovoltaic and photocatalytic properties by electrospinning', *ACS Appl. Mater. Interfaces*, 2012, **4**, (2), pp. 581–585

[12] Yang L., Li Z., Jiang H., *ET AL.*: 'Photoelectrocatalytic oxidation of bisphenol A over mesh of TiO_2/graphene/Cu_2O', *Appl. Catal. B Environ.*, 2016, **183**, pp. 75–85

[13] Li Y., Luo S., Wei Z., *ET AL.*: 'Electrodeposition technique-dependent photoelectrochemical and photocatalytic properties of an In_2S_3/TiO_2 nanotube array', *Phys. Chem. Chem. Phys.*, 2014, **16**, (9), pp. 4361–4368

[14] Daskalaki V.M., Antoniadou M., Li Puma G., *ET AL.*: 'Solar light-responsive Pt/CdS/TiO_2 photocatalysts for hydrogen production and simultaneous degradation of inorganic or organic sacrificial agents in wastewater', *Environ. Sci. Technol.*, 2010, **44**, (19), pp. 7200–7205

[15] Yang S.-M., Huang C.-H., Zhai J., *ET AL.*: 'High photostability and quantum yield of nanoporous TiO_2 thin film electrodes co-sensitized with capped sulfides', *J. Mater. Chem.*, 2002, **12**, (5), pp. 1459–1464

[16] Kang Q., Yang L., Chen Y., *ET AL.*: 'Photoelectrochemical detection of pentachlorophenol with a multiple hybrid $CdSe_xTe_{1-x}$/TiO_2 nanotube structure-based label-free immunosensor', *Anal. chemistry*, 2010, **82**, (23), pp. 9749–9754

[17] Park H., Choi W., Hoffmann M.R.: 'Effects of the preparation method of the ternary CdS/TiO_2/Pt hybrid photocatalysts on visible light-induced hydrogen production', *J. Mater. Chem.*, 2008, **18**, (20), pp. 2379–2385

[18] Yang L., Luo S., Liu R., *ET AL.*: 'Fabrication of CdSe nanoparticles sensitized long TiO_2 nanotube arrays for photocatalytic degradation of anthracene-9-carbonxylic acid under green monochromatic light', *J. Phys. Chem. C*, 2010, **114**, (11), pp. 4783–4789